

# Multi-Stage State of Health Estimation of Lithium-Ion Battery With High Tolerance to Heavily-Partial Charging

Zhongbao Wei, *Senior Member, IEEE*, Haokai Ruan, Yang Li, *Member, IEEE*, Jianwei Li, *Member, IEEE*, Caizhi Zhang, *Member, IEEE*, and Hongwen He, *Senior Member, IEEE*

**Abstract**—State of health (SOH) is critical to the management of lithium-ion batteries (LIBs) due to its deep insight into health diagnostic and protection. However, the lack of complete charging data is common in practice, which poses a challenge for the charging-based SOH estimators. This paper proposes a multi-stage SOH estimation method with a broad scope of applications, including the unfavorable but practical scenarios of heavily-partial charging. In particular, different sets of health indicators (HIs), covering both the morphological incremental capacity features and the voltage entropy information, are extracted from the partial CC charging data with different initial charging voltages to characterize the aging status. Following this endeavor, artificial neural network (ANN)-based HI fusion is proposed to estimate the SOH of LIB precisely in real-time. The proposed method is evaluated with long-term aging experiments performed on different types of LIBs. Results validate several superior merits of the proposed method, including high estimation accuracy, high tolerance to partial charging, strong robustness to cell inconsistency, and wide generality to different battery types.

**Index Terms**—state of health, health indicators, partial charging, lithium-ion battery

## I. INTRODUCTION

LITHIUM-ION batteries (LIBs) are frequently-used energy storage systems for electric vehicles (EVs) due to their unique merits of low-cost, high energy density, and strong reliability [1]. Despite the wide application, a meticulously-designed battery management system (BMS) is a prerequisite to guarantee the performance of the LIB system. Amongst others, the state of health (SOH) should be monitored accurately due to its property to depict the aging state of the battery [2].

SOH estimation has been incrementally recognized as a key functionality for BMS, giving rise to a myriad of methods that are generally categorized into model-based methods and data-based methods [3]. Model-based methods consider the battery

SOH as a state variable or a model parameter and update it with adaptive filters [4-6]. An alternative group of these methods tend to build the degradation model, based on which the SOH is estimated using the particle filter [7-9]. Although such architectures inherent high estimation accuracy, the sensitivity to the model accuracy and the vulnerability to the disturbance compromise its application in real scenarios [10, 11].

Data-based methods mitigate the faultiness and construct straightforward mapping relations to infer the SOH based on extracted health indicators (HIs) [12, 13]. The time interval [14] and voltage difference [15] are commonly-used HIs derived based on constant-current (CC) discharging mode, and they are very informative to infer SOH. However, the deviation of discharging mode discounts its adaptability in real applications. To remove such obstacles and potentiate online estimation at different discharge rates, a novel energy-based HI is developed by combining current with voltage sequence to infer SOH [16]. However, practical dynamic discharging conditions can lead to uncertain voltage differences within the same time interval, which impairs the precise evaluation of SOH [17].

In contrast, constant current-constant voltage (CCCV) charging attenuates practical uncertainties due to manufacturers' propensities to regular the charging mode. This has solicited increased interest and endeavors to use CCCV charging data to estimate the SOH of LIB. Time constant was extracted by exponentially fitting constant-voltage (CV) current and further utilized to infer the SOH [18]. Following a similar procedure, an equivalent circuit model (ECM) was employed to reflect the dynamic variation of CV current, and the aging factor was extracted to indicate the SOH [19]. Alternatively, regional CV charging current and CV duration were found to have a strong correlation with the battery capacity thus could be used for SOH estimation [14]. Although encouraging results validate the value of exploiting CV charging features, the need of complete CV charging is seldom fulfilled in practical applications since

Manuscript received July 17, 2021; revised December 15, 2021; accepted January 15, 2022. This work is supported by the National Natural Science Foundation of China under Grant 52072038. (Corresponding author: Yang Li.)

Zhongbao Wei, Haokai Ruan, Jianwei Li, and Hongwen He are with the National Engineering Laboratory for Electric Vehicles, School of Mechanical Engineering, Beijing Institute of Technology, Beijing, China. (e-mail: weizb@bit.edu.cn; 3220190306@bit.edu.cn; lijianw@bit.edu.cn; hwhebit@bit.edu.cn).

Yang Li is with the Department of Electrical Engineering, Chalmers University of Technology, 41296 Gothenburg, Sweden (e-mail: yangli@ieee.org).

Caizhi Zhang is with the School of Automotive Engineering, Chongqing University, Chongqing, China (e-mail: czhang@cqu.edu.cn).

Color versions of one or more of the figures in this article are available online at <https://ieeexplore.ieee.org>.

the CV charging phase is typically time-consuming, occupying the majority of the total charging time.

Instead, the CC charging phase, which recovers the majority of charge with much less time, also contains informative HIs for evaluating the SOH. The incremental capacity analysis (ICA) and differential voltage analysis (DVA) are the most used methods within this scope [20]. By comparison, the ICA has viewed wide applications due to the consistency of reference features [21]. Moreover, the IC indicators, i.e., the positions, heights, and areas of the IC peaks, have a direct linkage to the degradation process [22-24]. Despite the promising results, the IC curves are subject to noises induced by the differential operation, which hinders the extraction of HIs [25]. This has inspired enormous works on smoothing the IC curves [26]. The probability density function method was proposed to estimate the SOH [27]. To suppress the adverse effect of noises, an empirical model based on the deformed pseudo-Voigt peak function was used to fit the IC curve, and the extracted parameters were used to infer the phase transition behavior [28]. Gaussian/Lorentzian filter was employed to denoise the IC curves, and a strong correlation was found between the SOH and the shape of smoothed IC curve [29, 30]. Such methods inherit the merits of ICA and avoid tedious data preprocessing, but a complete charging profile is needed [31].

The integrity of the CC charging is hardly fulfilled in practice since the drivers tend to recharge the EVs before the LIBs are fully depleted. Estimation methods using partial CC segments are hence desired to tackle the uncertainty of the initial charging state. To this end, partial charging segments were used as the input of the support vector machine to estimate the battery SOH in [32]. The regional voltage was derived based on the partial CC phase and further applied to indicate the SOH in [33]. The charging duration between a fixed voltage interval was also found to have a strong correlation with the battery capacity thus could be used for SOH estimation [34, 35]. However, the use of a partial charging segment causes the loss of particular valuable HIs, which risks compromising the estimation accuracy.

This paper aims to bridge the aforementioned gaps and proposes a practical multi-stage SOH estimation method, which views a broad scope of applications, including the adverse but practical scenarios of heavily-partial charging. The major contributions of the paper are as follows:

1) IC-based HIs tend to disappear if the initial charging voltage exceeds particular regions. To mitigate this deficiency, the morphological IC features and voltage entropy information are extracted from the later/end stage of charging curves and are validated to be informative HIs within the high voltage plateau.

2) The extracted HIs are fused using the ANN model, giving rise to a universal multi-stage estimation method applicable to a broad scope of applications. The estimation performance of the proposed method under heavily-partial charging conditions is comparable to the case of using the ideal ICA with complete CC charging curves.

3) A comprehensive validation is performed based on the long-term aging experiments on three different types of LIB cells. The encouraging results validate the high fidelity, satisfied robustness, and generality of the proposed method.

The remainder of this article is organized as follows. Section II describes the experimental procedures and data set from different LIB cells. Section III elaborates the ANN-based multi-stage SOH estimator. The results are discussed in Section IV, while the main conclusions are summarized in Section V.

## II. EXPERIMENTAL DATASET

Three types of batteries from different data resources are adopted in this work, i.e., LiCoO<sub>2</sub> (LCO), LiNiCoAlO<sub>2</sub> (NCA), and blend of lithium cobalt oxide and lithium nickel cobalt oxide, and the corresponding testing procedures are described as follows.

From the open battery data source of the Center for Advanced Life Cycle Engineering (CALCE) at the University of Maryland, four LCO cells with a nominal capacity of 1.14 Ah, numbered #35, #36, #37, and #38, are selected for analysis. The cells are charged with the CCCV method, where the CC

### Experiment procedure

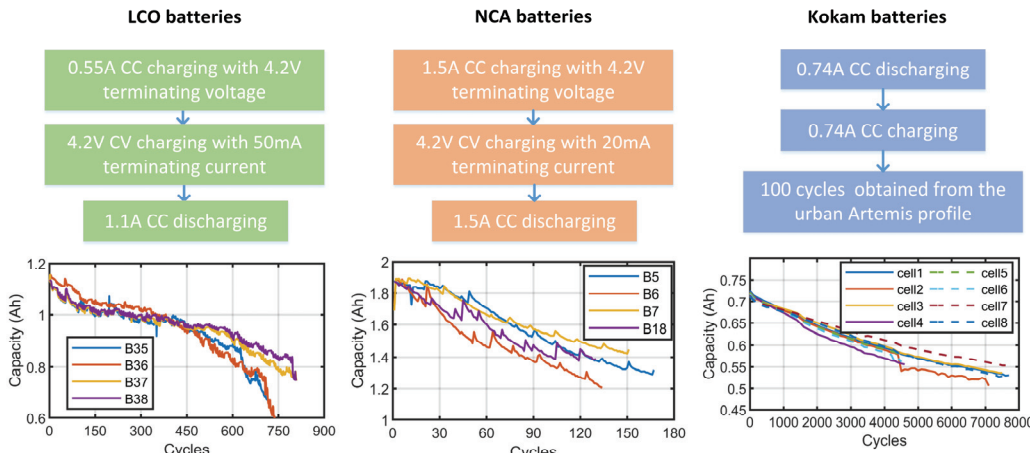


Fig. 1. Experiment procedure and capacity degradation curves of employed batteries.

current is 0.5 C, the upper voltage threshold is 4.2 V, while the CV terminal current is 50 mA. The cells are discharged with a constant current of 1C until the terminal voltage drops to 2.7 V. The test is conducted at room temperature of around 25 °C.

The NCA batteries from NASA Ames Prognostics Center of Excellence (PCoE), Moffett Field, CA, USA are charged with CCCV method at room temperature (around 25 °C), where the current at the CC stage is 1.5 A, the upper voltage threshold is 4.2 V, while the CV terminal current is 20 mA. The cells are discharged with 2 A until the terminal voltage drops to 2.7 V, 2.5 V, 2.2 V, and 2.5 V for B5, B6, B7, and B18, respectively. The cycling test is stopped when the reference capacity drops by 30%.

Based on the description of the Oxford Battery Degradation Dataset in [36], eight Kokam SLPB 533459H4 cells are tested at a constant temperature of 40 °C. The anode of the cell is graphite, and the cathode consists of lithium cobalt oxide and lithium nickel cobalt oxide. The cells are exposed to a CCCV charging profile, followed by the urban Artemis driving profile. 1C charge and 1C discharge are applied every 100 cycles to measure the characteristic.

The equipment used to conduct the aging tests of LIBs is shown in Fig. 2. It includes an Arbin LBT21014 tester to charge/discharge batteries, a thermal chamber to control battery temperatures, and a computer for data monitoring and storage.

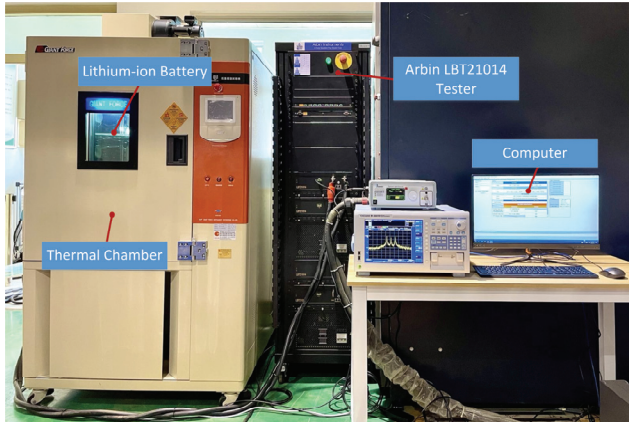


Fig. 2. Battery test equipment.

### III. MULTI-STAGE SOH ESTIMATION

In this section, an ANN-based multi-stage SOH estimator is elaborated by using the LCO battery numbered #35 from CALCE as an example.

#### A. IC-based HI Extraction

IC curve is derived by associating the incremental capacity with the elevated voltage based on CC charging data. The IC curve contains many informative HIs highly relevant to the health state of LIB, thus has been widely used for the SOH estimation of LIB. However, the direct derivation of discrete voltage data leads to a highly noisy raw IC curve (blue plots in Fig. 3), which hinders the extraction of HIs. To remedy this defect, in this paper, the Gaussian function is employed as a filter to eliminate the heavy noises before usable HIs are

extracted. Based on the Gaussian function, the  $dQ/dV$  as a function of the terminal voltage can be expressed by:

$$\frac{dQ}{dV} = \sum_{i=1}^n \sqrt{\frac{2}{\pi}} \frac{A_i}{\omega_i} \exp\left(-2\left(\frac{V - V_{0i}}{\omega_i}\right)^2\right) \quad (1)$$

where  $n$  is the number of peaks,  $A_i$  is the area below the  $i_{th}$  peak,  $\omega_i$  represents the peak width of  $i_{th}$  peak,  $V_{0i}$  is the symmetry center of  $i_{th}$  peak.  $A_i$ ,  $\omega_i$  and  $V_{0i}$  are the parameters to be identified, and  $n$  takes different values according to the battery chemical materials. However, numerous noises or spikes of the raw IC curve invalidate the identification of parameters. Thus the integration is performed to Gauss function to fit a relatively smooth  $Q$ - $V$  curve:

$$Q = \sum_{i=1}^n \frac{-A_i}{2} \operatorname{erf}\left(\frac{\sqrt{2}(V_{0i} - V)}{\omega_i}\right) + C \quad (2)$$

with

$$\operatorname{erf}(x) = \frac{2}{\sqrt{\pi}} \int_0^x e^{-\eta^2} d\eta \quad (3)$$

Although the raw  $Q$ - $V$  curve seems to coincide with the filtered  $Q$ - $V$  curve, the IC curve based on the differential of the raw  $Q$ - $V$  curve contains extremely strong noise. Therefore, it is not possible to extract the peak features directly from the raw IC curve. The proposed  $Q$ - $V$  fitting-based filtering can promise the direct extraction of informative HIs with the raw current-voltage data readily available from the battery management systems.

The parameters identification is conducted using the nonlinear least-squares method based on the measured  $Q$ - $V$  curve. During the identification process, it is necessary to constrain the range of parameters, as shown in Table I. Through this endeavor, the easily-extracted IC peaks can be obtained from the hardly-identifiable voltage region on the  $Q$ - $V$  curve. The filtered  $Q$ - $V$  curve and IC curve against their raw versions are shown in Fig. 3. It can be seen that the three peaks exist on the IC curve located in the area nearby 3.8 V, 3.9 V, and 4.0 V, respectively. The fitted  $Q$ - $V$  curve closely follows the measured one while the large disturbances are filtered out effectively.

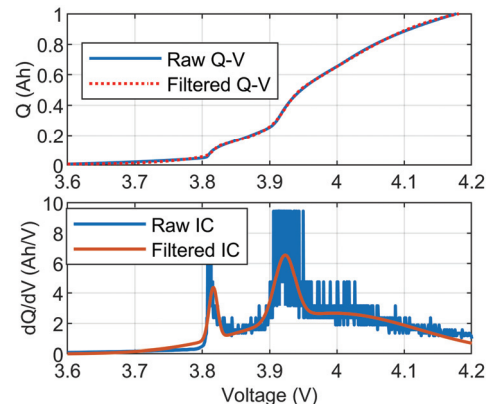


Fig. 3. Raw and filtered  $Q$ - $V$  and IC curves.

TABLE I  
RANGE OF PARAMETERS IN GAUSSIAN FUNCTION

Parameters	Lower limit	Upper limit
$A_i$ (Ah)	0	4
$V_{oi}$ (V)	3.7	4.2
$\omega_i$ (V)	0	2

The drift of voltage curves during the CC phase and the IC curves with the cyclic usage are shown in Fig. 4. This motivates using the nine parameters in Table I as effective HIs. To justify this, the relationships between these parameters and the battery capacity are shown in Fig. 5. All the HIs shown in Fig. 5 are selected to indicate the battery SOH since the heights, width, and areas of IC peaks have the potential to quantitatively evaluate the loss of lithium-ions and active materials, which is highly related to inferring SOH [4, 5]. Moreover, the corresponding correlation coefficients are listed in Table II. The exhibited strong correlations further confirm the suitability of using the nine extracted parameters as HIs to estimate the SOH of LIB.

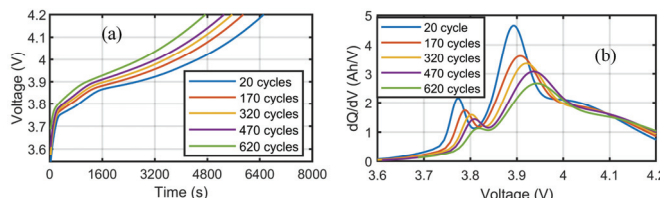


Fig. 4. Curves with cyclic usage: (a) CC charging curves and (b) IC curves.

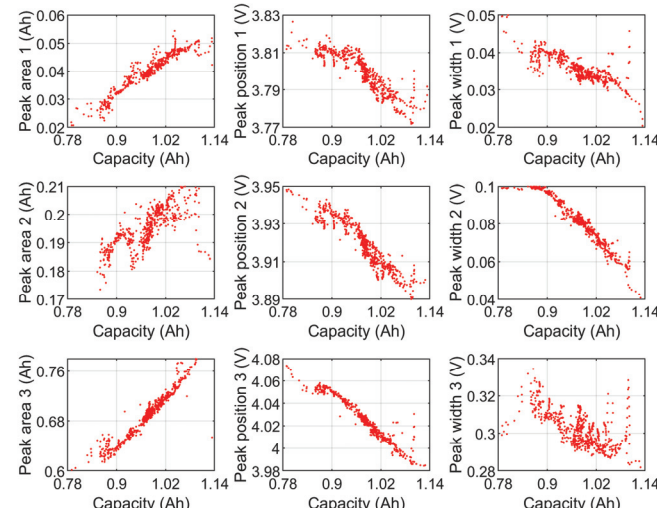


Fig. 5. Change of extracted IC-based HIs against the battery capacity.

TABLE II  
CORRELATION COEFFICIENTS BETWEEN IC-BASED HIs AND THE BATTERY CAPACITY

Parameters	Peak 1	Peak 2	Peak 3
$A_i$ (Ah)	0.9475	0.7800	0.9721
$V_{oi}$ (V)	0.9055	0.9504	0.9702
$\omega_i$ (V)	0.7891	0.9544	0.5840

### B. Effect of Initial Charging Voltage

EVs are commonly recharged before the batteries deplete to a low state of charge (SOC). Thus, complete CC charging is seldom available in real applications. This can lead to the loss of IC-based HIs. Particularly, as shown in Fig. 4(b), only the

third peak can be retained if the charging is started at a high voltage, e.g., within the region from 4 V to 4.2 V. In other words, several informative HIs disappear due to the incomplete CC charging, which inevitably discounts the accuracy of SOH estimation.

With respect to the IC-based HI extraction in Section III-A, the elevated initial charging voltage means less charging data for fitting the  $Q$ - $V$  curve, which potentially discounts the parameter identification. It is shown in Fig. 6 that the mean absolute error (MAE) of  $Q$ - $V$  fitting remains around 4 mV at the low-voltage region and increases once the initial charging voltage exceeds 4.03 V. Therefore, the initial charging voltage ranged from 4 V – 4.2 V can be identified as a “dangerous region” where the IC-based HI extraction loses effect.

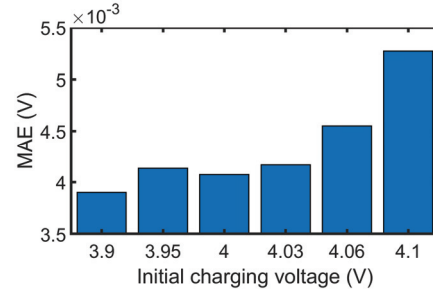


Fig. 6. MAE of  $Q$ - $V$  curve fitting with different initial charging voltage.

### C. HI Extraction under Heavily-Partial Charging

As discussed, new useful HIs should be found to address the heavily-partial charging scenario where the initial charging voltage reaches 4V.

It is obvious that CC charging duration occupies less time with the cyclic usage as shown in Fig. 4(a), thus the regional charging duration  $T_{RCC}$  is considered to be a promising HI to estimate the battery SOH. Moreover,  $T_{RCC}$  can be easily extracted without extra computations, which appeals to real-time implementation. However, it is found that for the high voltage plateau, the  $T_{RCC}$  - SOH correlation is not sufficiently strong to support a precise estimation compared to the IC features. This is particularly true for cells with different initial aging statuses, as described in Section II. To solve the pre-mentioned issues, other indicators should be introduced for quantifying the change of the curves to further improve the estimation accuracy.

As observed in Fig. 4(a), the voltage increased more rapidly with the battery aging. To this end, entropy is an efficient feature describing the chaotic degree of time-series data that has been used for SOH estimation [39, 40]. However, the entropy is sensitive to the noise since it uses a step function to calculate the similarity degree [41]. Fuzzy entropy (FE) improves the entropy by replacing the step function with the exponential function (corresponding to **Step 3** in Table III) and become more robust to the disturbances [42]. Hence, the FE is employed to evaluate the rising rate of charging voltage, which is expected to be indicative of SOH estimation. Compared to the traditional entropy and sample entropy, FE can quantify the data regularity based on the exponential function, which has a more detailed

description of voltage variation. Moreover, the FE-based method possesses several advantages manifesting itself as a good HI, i.e., anti-noise capability, less data demand, and strong robustness to different aging conditions. Therefore, fuzzy entropy calculation is based on the raw voltage data, and the detailed algorithm of FE is described in Table III.

The selection of  $m$  and  $r$  herein should be determined beforehand, depending on the specific battery type. In this regard,  $m$  is commonly selected as 2 or 3, and  $r$  is set between 0.1 and 0.25 times the standard deviation of the data [43]. Then, appropriate results can be derived according to the minimum relative error of the maximum fuzzy entropy.

$T_{RCC}$  and FE represent the regularity of the time-series voltage curve on the transverse axis and longitudinal axis of Fig. 5 (a). Combined with the three features of the third peak on the IC curve, five HIs are fused for SOH estimation, with the expectation to tackle the adverse scenario with heavy CC partialness when the initial charging voltage is over 4 V.

TABLE III  
DETAILED PROCEDURES TO DETERMINE THE FE OF CHARGING VOLTAGE

Initialization of parameter vector  $\mathbf{m}$ ,  $\mathbf{r}$ , and  $\mathbf{n}$

**Step 1:** Dividing voltage series of CC phase  $\{V_i, i = 1, 2, \dots, n\}$  into  $k = n - m + 1$  sequences  $v_i = (V_i, V_{i+1}, \dots, V_{i+m})$  by using  $m$  as the window size;

**Step 2:** Calculate the distance between each sequence and all the other sequences, and the distance is the maximum absolute value of the difference between the corresponding elements of the two vectors  $d_{ij} = \max|v_i(t)-v_j(t)|$ ;

**Step 3:** The fuzzy membership degree  $D$  is calculated according to the distance  $d$

$$D_{ij}^m = \mu(d_{ij}^m, n, r) = \exp\left(-\frac{(d_{ij}^m)^n}{r}\right)$$

Calculate the mean value of all membership degrees except itself

$$\Phi^m(n, r) = \frac{1}{n-m} \sum_{j=1}^{n-m} \left[ \frac{1}{n-m-1} \sum_{j=1, j \neq i}^{n-m} D_{ij}^m \right]$$

**Step 4:** Increase  $m$  to  $m + 1$  and repeat **Step 1** to 3

**Step 5:** Calculating fuzzy entropy

$$FE = \ln \Phi^m - \ln \Phi^{m+1}$$

Since drivers plan the charging of EVs based on the battery's remaining charge, it is useful to map the charging voltage to SOC to reflect this practice. Therefore, SOC values corresponding to the voltage from 4 V to 4.2 V are plotted against the life cycles in Fig. 7. It can be observed that the charging voltage of 4 V and 4.05 V correspond to the SOC range of [40%, 65%] and [50%, 70%] approximately during the lifetime of LIB. Therefore, it is most probable that the charging of the LIB system will start from these SOC regions. By comparison, the charging voltage of 4.1 V means high SOC charging within the range of [65%, 80%] for most of the lifetime. To this end, initial charging voltage over 4.1 V is not a common case in real-world charging operations. Even if such high-SOC charging happens regularly in practical applications, it is reasonable to abandon such cycles for estimation. This is because the aging is quite slow during the long service time of the LIB system, and the discard of limited high-voltage charging cycles does not necessarily deteriorate the life diagnostic. When the voltage exceeds 4.1 V, most of the IC

peak features are lost due to the heavily-partial charging curve. In this case, only the fuzzy entropy and regional charging time can serve as the health indicator. Therefore, the charging curve beginning from extremely-high SOC is not suggested for use in the proposed method.

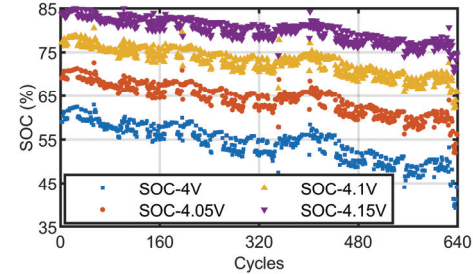


Fig. 7. The SOCs over the lifetime of the battery with different initial charging voltages.

#### D. HI Fusion and SOH Estimation

The sophisticated electrochemical process leads to highly nonlinear characteristics of LIB, which challenges the accurate estimation of SOH with a single HI. Therefore, an ANN model is employed to fusion HIs belonging to different categories and to estimate the SOH. The neural networks utilized to estimate SOH are both the back-propagation neural network (BPNN). The ANN 1 consists of one input layer with 9 neurons, two hidden layers with 10 and 8 neurons, and one output layer with 1 neuron. The ANN 2 consists of one input layer with 5 neurons, two hidden layers with 8 and 10 neurons, and one output layer with 1 neuron. Combining the characteristic of multi-stage calculation and multi-category HI fusion, the proposed SOH estimation method is shown schematically in Fig. 8. The detailed procedures are summarized in Table IV.

TABLE IV  
DETAILED PROCEDURES OF THE PROPOSED SOH ESTIMATION METHOD

##### Model training (offline):

**Step 1-1:** Based on the complete CC charging curve, the capacity-voltage data is fitted by the gaussian function. The extracted 9 parameters, i.e.,  $A_1, \omega_1, V_{01}, A_2, \omega_2, V_{02}, A_3, \omega_3$ , and  $V_{03}$ , are treated as the input to train the ANN model. The trained model is named ANN 1;

**Step 1-2:** Based on charging data within the charging voltage range [4.1V, 4.2V],  $T_{RCC}$  and FE combined with the parameters of the third peak in the IC curve, i.e.,  $A_3, \omega_3$ , and  $V_{03}$ , are extracted and employed to train the ANN model. The trained model is named ANN 2.

##### Practical SOH estimation (online):

**Step 2-1:** If the initial charging voltage is 4.0 V or lower, the 9 HIs in Step 1-1 are extracted from the relatively-complete IC curves and fed to the trained ANN 1 for SOH estimation.

**Step 2-2:** If the initial charging voltage is between 4.0 V and 4.1 V, the five HIs in Step 1-2, i.e., FE,  $T_{RCC}$ ,  $A_3$ ,  $\omega_3$ , and  $V_{03}$ , are extracted and fed to the trained ANN 2 for SOH estimation.

**Step 2-3:** If the initial charging voltage is higher than 4.1 V, the estimation is not adopted.

## IV. RESULTS AND DISCUSSION

Following the procedures summarized in Fig. 8, in this section, the proposed SOH estimation method is validated under typical scenarios with different degrees of charging partialness on multiple battery types.

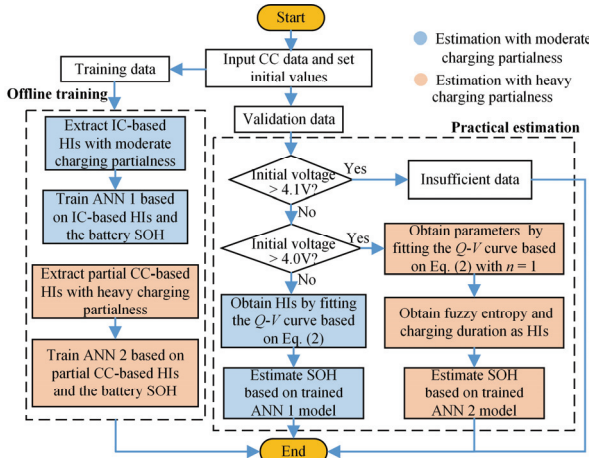


Fig. 8. The framework of the proposed SOH estimation method.

#### A. Validation with Moderate Charging Partialness

ANN 1 model is established to cope with the scenario of moderately-partial CC charging herein, with an initial voltage of 4.0 V. Battery #35 is utilized for training the model, and batteries #36, #37, and #38 are used for validation. The estimation results obtained from the trained cell are shown in Fig. 9(a). It is shown that the estimates of SOH agree with the experimental benchmarks closely, and most estimation errors are within an error bound of  $\pm 3\%$ . Furthermore, as suggested by Table V, the MAE of estimation is as low as 0.24%. The encouraging results validate that the proposed method can estimate the SOH of the training cell with high accuracy.

Despite the same chemical composition, the performances of the cell may deviate from each other in the manufacturing process. The cell inconsistency can also enlarge significantly with the aging of the battery, which causes inconsistent results by using different batteries. Deviation also emerges from the model training since the model depends on the training data. Higher accuracy is expected if the new cell characteristics are close to the trained cell. It is unrealistic to train the ANN model for every cell in practice. Therefore, the model trained for a single cell should have the robustness to be utilized for other cells. In this regard, the trained model is used to estimate the SOH of batteries #36, #37, and #38, and the results are shown in Fig. 9(b)-(d). As shown, the estimated SOHs resemble the experimental degradation trajectories tightly throughout the lifetime of investigated LIBs. Referring to the first row in Table V, it is not surprising that the estimation errors build up to some extent on the new cells due to cell inconsistency. However, the observed MAEs (within 1%) are still quite satisfactory from the online estimation point of view. Results suggest that the trained ANN model can be well generalized to new cells, which validates the robustness of the proposed method against the cell consistency.

Experiments are repeated under different initial charging voltages, i.e., 3.85 V and 3.7 V. The estimation results are summarized in the second and third rows of Table V. As can be observed, consistent results can be obtained from the two cases. The estimation mismatches have been well confined to a low level, suggesting the high fidelity of the proposed method for SOH estimation with moderately partial CC charging data.

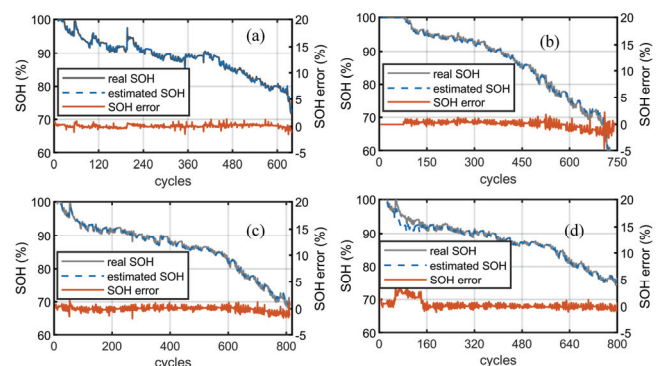


Fig. 9. Estimation results on LCO batteries with moderately-partial charging: (a) B35, (b) B36, (c) B37 and (d) B38.

TABLE V  
MAEs OF SOH ESTIMATION WITH DIFFERENT INITIAL CHARGING VOLTAGES (LCO BATTERIES,  $\leq 4$  V)

Initial charging voltage	B35	B36	B37	B38
4 V	0.24%	0.72%	0.54%	0.78%
3.85 V	0.36%	0.80%	0.64%	0.82%
3.7 V	0.24%	0.60%	0.66%	0.77%

#### B. Validation with Heavy Charging Partialness

This section scrutinizes the performance of ANN 2 under more adverse scenarios with heavy charging partialness, where the initial charging voltage lays within the range of 4 V – 4.1 V, corresponding to the SOC range of 40% – 80%. Referred to the procedures shown in Fig. 8, FE,  $T_{RCC}$ ,  $A_3$ ,  $\omega_3$ , and  $V_{03}$  are extracted as HIs for SOH estimation. ANN 2 model is trained by battery #35, and batteries #36, #37, and #38 are used for validation. The estimation results are shown in Fig. 10, and the statistical errors with different initial charging voltages are summarized in Table VI.

It shows that even though only heavily-partial charging data are available, the estimated SOHs are still in good agreement with the ground truth during the entire life cycle for both the trained and the new cells. Referring to Table VI, the MAEs of estimation lay in a low spectrum covering the range from 0.34% to 0.85%. The estimation error is enlarged only slightly, if observable, compared to the results in Section IV-A. Even at a quite tough scenario that the initial voltage reaches 4.1 V, corresponding to an initial charging SOC within [65%, 80%], the SOH can be estimated precisely with the MAE confined to the level of around 1%. In other words, the much-aggregated charging partialness does not necessarily skew the estimation performance, attributed to the embodiment of multi-stage and multi-category feature fusion.

TABLE VI  
MAEs OF SOH ESTIMATION WITH DIFFERENT INITIAL CHARGING VOLTAGES (LCO BATTERIES, 4 V–4.1 V)

Initial charging voltage	B35	B36	B37	B38
4.1 V	0.34%	0.57%	0.35%	0.85%
4.06 V	0.33%	0.91%	0.53%	0.81%
4.03 V	0.33%	0.73%	0.52%	1.23%

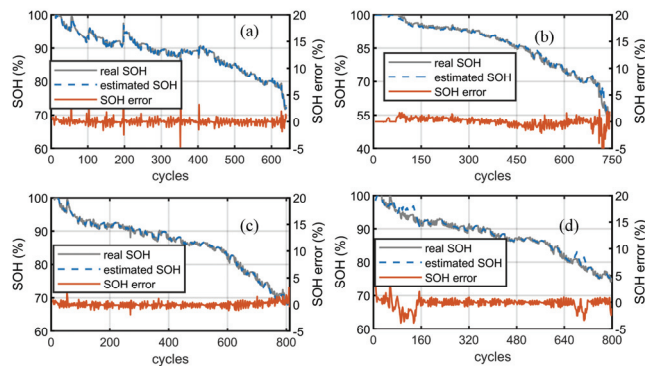


Fig. 10. Estimation results on LCO batteries with heavily-partial charging: (a) B35, (b) B36, (c) B37, and (d) B38.

### C. Generality to Different Battery Types

The successful application of the proposed method on LCO batteries motivates its versatility to other types of batteries. Validation is performed on the NCA batteries as described in Section II. Under the scenario of moderately-partial charging, ANN 1 model is trained afresh based on battery #5, and batteries #6, #7, and #18 are used for validation. The estimated SOHs are plotted against their benchmarked values in Fig. 11, and the corresponding statistical errors are summarized in Table VII. Similar to the case of LCO batteries, the proposed estimation method attains very close results to the acausal benchmarks. The MAEs are generally within 2%.

Considering more adverse scenarios of heavily-partial charging, FE,  $T_{RCC}$ ,  $A_3$ ,  $\omega_3$ , and  $V_{03}$  are extracted as HIs feeding into ANN 2 for SOH estimation. The model is trained by battery #5, and batteries #6, #7, and #18 are used for validation. The SOH estimation results are shown in Fig. 12, while the statistical errors are summarized in Table VIII. It is not surprising that the mismatch generally builds up compared to the earlier case since the heavy charging partialness hinders the extraction of valuable aging information. However, even in a tough scenario that the initial charging voltage reaches 4.1 V, the SOH can be estimated authentically with the MAE confined to approximately 2%. This validates that the proposed method is efficient for different degrees of charging partialness. The performance of the proposed method on NCA batteries is hence validated.

TABLE VII  
MAEs OF SOH ESTIMATION WITH DIFFERENT INITIAL CHARGING VOLTAGES  
(NCA BATTERIES,  $\leq 4$  V)

Initial charging voltage	B5	B6	B7	B18
4 V	0.3%	2.54%	1.21%	1.17%
3.9 V	1.04%	1.5%	2.00%	1.37%
3.8 V	0.3%	1.96%	0.78%	1.65%

TABLE VIII  
MAEs OF SOH ESTIMATION WITH DIFFERENT INITIAL CHARGING VOLTAGES  
(NCA BATTERIES, 4 V–4.1 V)

Initial charging voltage	B5	B6	B7	B18
4.1 V	1.10%	1.32%	1.77%	1.36%
4.06 V	0.66%	1.53%	1.77%	2.01%
4.03 V	0.43%	1.71%	1.00%	1.65%

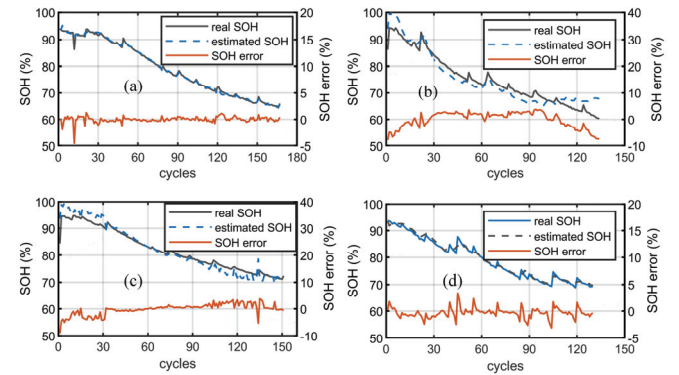


Fig. 11. Estimation results on NCA batteries with moderately-partial charging: (a) B5, (b) B6, (c) B7, and (d) B18.

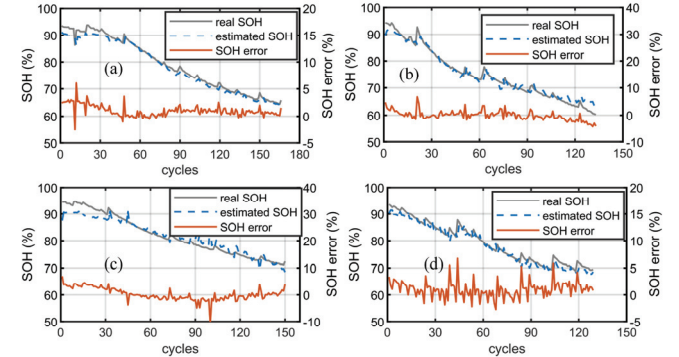


Fig. 12. Estimation results on NCA batteries with heavily-partial charging: (a) B5, (b) B6, (c) B7, and (d) B18.

The proposed method is further performed on Kokam pouch cells of the Oxford dataset. Similarly, IC-based HIs are extracted to infer the SOH based on ANN 1 under the moderately-partial charging scenario. The model is trained by cell #1 and validated on the other seven cells. As shown in Fig. 13, the estimated SOHs agree with the measured ones closely, and the corresponding MAEs are confined below 1.5%, as referred to in Table IX. For the scenario of heavily-partial charging, the estimation results are shown in Fig. 14, ANN 2 model is trained by cell #1 and validated on the other seven cells, and the statistical errors are listed in Table X. Not surprisingly, the mismatch increases due to the heavier partialness of the charging curve. Nevertheless, the estimates are generally within an error bound of  $\pm 3\%$ , and the MAEs are within 2.5% except for a few outliers with different initial charging voltages. Hence, it is validated that the proposed method is highly authentic for application on Kokam cells.

A comparison between the proposed method and existing state-of-the-art techniques is listed in Table XI. It can be observed that the proposed method has lower MAEs than state-of-the-art algorithms except for the results of the Oxford dataset based on ANN and ELM. However, it is worth noting that the results of the proposed method are obtained under much more harsh/practical conditions where only heavily-partial charging curves are available (initial voltage of 4.1 V). By comparison, the results from other methods are obtained under ideal conditions where complete charging data are available. In summary, the proposed method contributes to improving the

SOH estimation accuracy with much less charging data. This appeals well to practical charging utilization since complete charging data are hardly available.

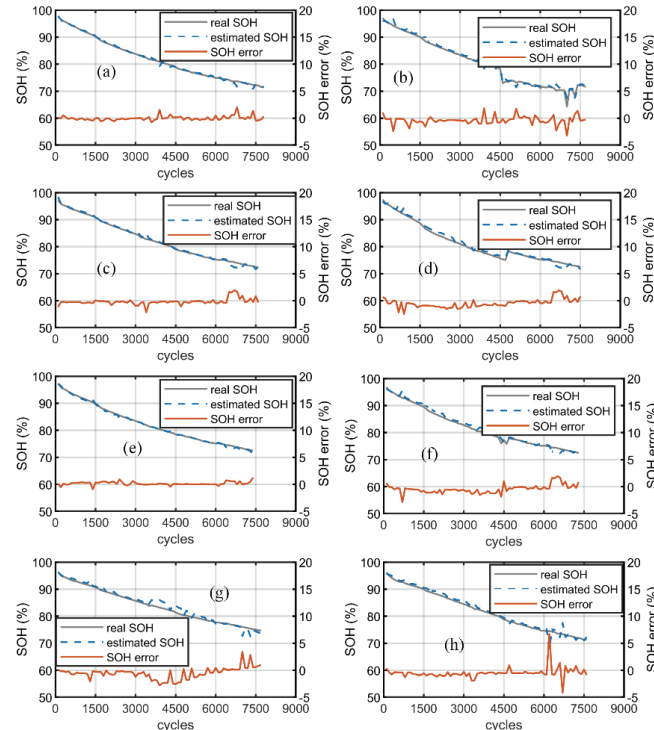


Fig. 13. Estimation results on Kokam batteries under moderately-partial charging scenario: (a)-(h) Cell 1-8.

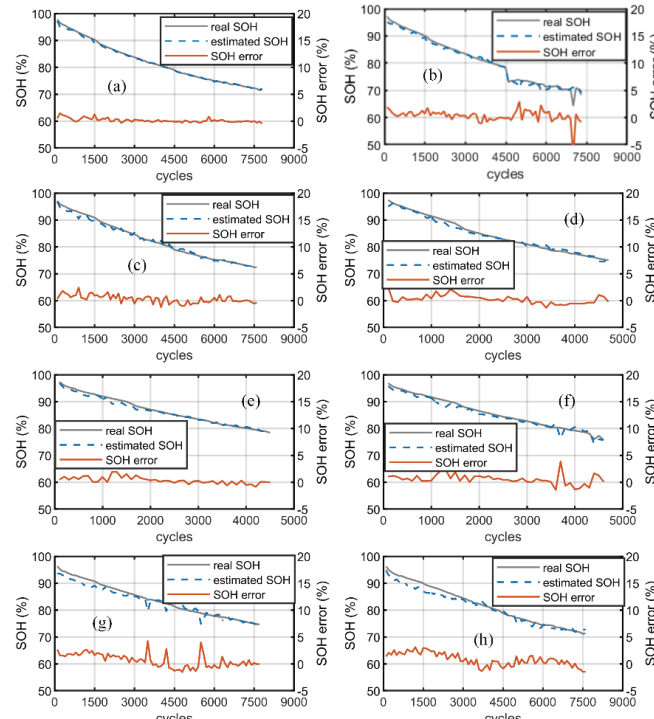


Fig. 14. Estimation results on Kokam batteries under heavily-partial charging scenario: (a)-(h) Cell 1-8.

TABLE IX  
MAEs OF SOH ESTIMATION WITH DIFFERENT INITIAL CHARGING VOLTAGES (KOKAM BATTERIES,  $\leq 4$  V)

Initial charging voltage	Cell 1	Cell 2	Cell 3	Cell 4
4 V	0.20%	0.97%	0.60%	0.69%
	0.20%	1.31%	1.43%	1.21%
	0.42%	1.04%	1.15%	0.90%
3.85 V	0.84%	0.82%	0.98%	1.32%
	1.34%	1.23%	1.94%	0.85%
	0.89%	0.64%	1.46%	0.81%
3.7 V	0.42%	1.04%	1.15%	0.90%
	1.04%	1.15%	0.90%	
	0.89%	0.64%	1.46%	0.81%

TABLE X  
MAEs OF SOH ESTIMATION WITH DIFFERENT INITIAL CHARGING VOLTAGES (KOKAM BATTERIES, 4V–4.1V)

Initial charging voltage	Cell 1	Cell 2	Cell 3	Cell 4
4.1 V	0.37%	1.62%	0.93%	1.10%
	0.42%	2.48%	1.62%	1.83%
	0.46%	2.02%	1.92%	2.43%
4.06 V	1.58%	1.10%	1.74%	1.87%
	1.54%	2.57%	1.49%	2.11%
	1.38%	2.12%	1.95%	2.84%
4.03 V	0.46%	2.02%	1.92%	2.43%
	1.58%	1.10%	1.74%	1.87%
	1.54%	2.57%	1.49%	2.11%

TABLE XI  
COMPARISON OF SOH ESTIMATION ACCURACY

Method	Battery	Data requirement	MAE
SVR [25]	NASA	3.8 V-4 V	$\leq 2.49\%$
	Oxford	3.6 V-3.8 V	$\leq 3.62\%$
ANN [44]	CALCE	3.9 V-4.2 V	$\leq 2.90\%$
	Oxford	3.7 V-4.2 V	$\leq 1.796\%$
ELM [45]	CALCE	3.9 V-4.2 V	$\leq 2.43\%$
	Oxford	3.8 V-4.2 V	$\leq 0.69\%$
Proposed method	CALCE	4.1 V-4.2 V	$\leq 0.85\%$
	NASA	4.1 V-4.2 V	$\leq 1.77\%$
	Oxford	4.1 V-4.2 V	$\leq 1.87\%$

Summarized from the above results, the proposed method promises a five-fold benefit, i.e., a high estimation accuracy, low demand on the integrity of CC charging, strong robustness to cell inconsistency, a broad generality to different battery types, and a foreseeable low computing cost attributed to the use of simple ANN model for HI fusion.

#### D. Discussion

The SOH estimation has been validated with high accuracy and high generality to different battery chemistries. However, it is worth noting that the encouraging results are obtained from the conditions with stable charging current and temperature. In more adverse conditions, the change of charging current and temperature can discount the accuracy of the proposed method since they can cause the mitigation and distortion of IC curves.

To address this problem, an OCV model has been proposed in our previously-published work to compensate for the potential impact of charging current and temperature [7]. By using the compensated charging curve, the SOH has been validated to be estimated precisely. It will be a good practice to incorporate the OCV model within the proposed estimation framework to improve the feasibility of estimation further. This will be a research topic to explore in our future work.

Considering the computational demand in the training process, a vehicle-to-cloud framework is established for the

training and implementation of ANN-based SOH estimator, as shown in Fig. 15.

The charging data is collected based on the battery sensors generating the application-oriented charging profiles to the cloud platform. According to the pre-determined voltage threshold, the logged data are classified into moderately-partial charging and heavily-partial charging, which are utilized for training model ANN 1 and model ANN 2, respectively. Once the training process is accomplished, parameters of the trained model can be transmitted to the BMS in EVs to perform the SOH estimation based on the practical charging data.

The cloud-based training approach is proposed with real-world data collected from batteries with different chemical materials, which equips the SOH estimator with low-cost BMS, robust to practical scenarios, and broad generality to different battery types.

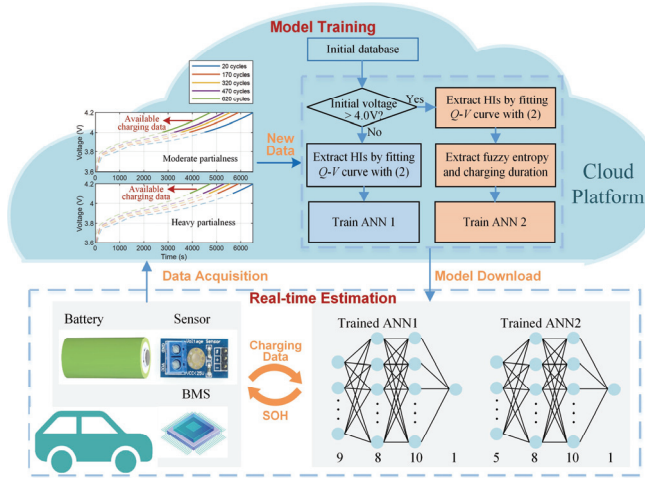


Fig. 15. The framework of cloud-based SOH estimation.

## V. CONCLUSIONS

This paper proposes a multi-stage SOH estimation method with high tolerance to the adverse but practical scenarios of heavily-partial charging. Different sets of HIs are extracted from the partial CC charging data depending on the initial charging voltage. The HIs are further fused using ANN to estimate the battery SOH in real-time. Long-term degradation experiments have been performed on LCO, NCA, and Kokam pouch cells for method validation. The primary conclusions are summarized as follows:

1) The fuzzy entropy and regional charging time validate to supplement the loss of IC features in heavily-partial scenarios. This is validated by the equivalent accuracy compared to the case of using complete charging data.

2) The proposed method has a high tolerance to the practical partial charging condition. The MAEs of SOH estimation are less than 1.23% even in an adverse case where the initial charging voltage lies within 4 V–4.1 V (a SOC range of 40%–80%).

3) The proposed method has a strong robustness to the cell inconsistency, validated by the observed high estimation accuracy on both the trained and tested LIBs.

4) This method is robust to different types of batteries. The MAEs are confined in the range from 0.3% to 2.54% for NCA cells and 0.2% to 2.84% for eight Kokam pouch cells.

## REFERENCES

- [1] Y. Shang, S. Zhao, Y. Fu, B. Han, P. Hu, and C. C. Mi, "A lithium-ion battery balancing circuit based on synchronous rectification," *IEEE Trans. Power Electron.*, vol. 35, no. 2, pp. 1637-1648, 2020.
- [2] A. E. Mejdoubi, H. Chaoui, H. Gualous, P. Bossche, and J. V. Mierlo, "Lithium-ion batteries health prognosis considering aging conditions," *IEEE Trans. Power Electron.*, 2018.
- [3] X. Hu, H. Yuan, C. Zou, Z. Li, and L. Zhang, "Co-estimation of state of charge and state of health for lithium-ion batteries based on fractional-order calculus," *IEEE Trans. Veh. Technol.*, vol. 67, no. 11, pp. 10319-10329, 2018.
- [4] Z. Song, H. Wang, J. Hou, H. F. Hofmann, and J. Sun, "Combined state and parameter estimation of lithium-ion battery with active current injection," *IEEE Trans. Power Electron.*, vol. 35, no. 4, pp. 4439-4447, 2020.
- [5] D. Xiao, G. Fang, S. Liu, S. Yuan, and A. Emadi, "Reduced-coupling co-estimation of SOC and SOH for lithium-ion batteries based on convex optimization," *IEEE Trans. Power Electron.*, vol. 35, no. 11, pp. 12332-12346, Nov. 2020.
- [6] Z. Wei, J. Zhao, R. Xiong, G. Dong, J. Pou, and K. J. Tseng, "Online estimation of power capacity with noise effect attenuation for lithium-ion battery," *IEEE Trans. Ind. Electron.*, vol. 66, pp. 5724-5735, 2018.
- [7] G. Dong, Z. Chen, J. Wei, and Q. Ling, "Battery health prognosis using Brownian motion modeling and particle filtering," *IEEE Trans. Ind. Electron.*, vol. 65, no. 11, pp. 8646-8655, 2018.
- [8] X. Cong, C. Zhang, J. Jiang, W. Zhang, Y. Jiang, and X. Jia, "An improved unscented particle filter method for remaining useful life prognostic of lithium-ion batteries with  $\text{Li}(\text{NiMnCo})\text{O}_2$  cathode with capacity diving," *IEEE Access*, vol. 8, pp. 58717-58729, 2020.
- [9] Z. Lyu, R. Gao, and L. Chen, "Li-Ion battery state of health estimation and remaining useful life prediction through a model-data-fusion method," *IEEE Trans. Power Electron.*, vol. 36, no. 6, pp. 6228-6240, 2021.
- [10] K. Liu, Y. Shang, Q. Ouyang, and W. D. Widanage, "A data-driven approach with uncertainty quantification for predicting future capacities and remaining useful life of lithium-ion battery," *IEEE Trans. Ind. Electron.*, vol. 68, no. 4, pp. 3170-3180, 2021.
- [11] Z. Wei, H. He, J. Pou, K.-L. Tsui, Z. Quan, and Y. Li, "Signal-disturbance interfacing elimination for unbiased model parameter identification of lithium-ion battery," *IEEE Trans. Ind. Informat.*, 2020.
- [12] J. Meng *et al.*, "An automatic weak learner formulation for lithium-ion battery state-of-health estimation," *IEEE Trans. Ind. Electron.*, vol. 69, no. 3, pp. 2659-2668, Mar. 2022.
- [13] H. Ruan, H. He, Z. Wei, Z. Quan, and Y. Li, "State of health estimation of lithium-ion battery based on constant-voltage charging reconstruction," *IEEE J. Emerg. Sel. Topics Power Electron.*, 2021.
- [14] Y. Wu, Q. Xue, J. Shen, Z. Lei, Z. Chen, and Y. Liu, "State of health estimation for lithium-ion batteries based on healthy features and long short-term memory," *IEEE Access*, vol. 8, pp. 28533-28547, 2020.
- [15] D. Liu, J. Zhou, H. Liao, Y. Peng, and X. Peng, "A health indicator extraction and optimization framework for lithium-ion battery degradation modeling and prognostics," *IEEE Trans. Syst., Man, Cybern. Syst.*, vol. 45, no. 6, pp. 915-928, 2015.
- [16] W. Liu and Y. Xu, "Data-driven online health estimation of Li-ion batteries using a novel energy-based health indicator," *IEEE Trans. Energy Convers.*, vol. 35, no. 3, pp. 1715-1718, 2020.
- [17] Z. Deng, X. Hu, X. Lin, L. Xu, Y. Che, and L. Hu, "General discharge voltage information enabled health evaluation for lithium-ion batteries," *IEEE/ASME Trans. Mechatronics*, 2020.
- [18] J. Wei, G. Dong, and Z. Chen, "Remaining useful life prediction and state of health diagnosis for lithium-ion batteries using particle filter and support vector regression," *IEEE Trans. Ind. Electron.*, vol. 65, no. 7, pp. 5634-5643, 2018.
- [19] Z. Wang, S. Zeng, J. Guo, and T. Qin, "State of health estimation of lithium-ion batteries based on the constant voltage charging curve," *Energy*, vol. 167, pp. 661-669, 2019.
- [20] J. He, Z. Wei, X. Bian, and F. Yan, "State-of-health estimation of lithium-ion batteries using incremental capacity analysis based on

- voltage–capacity model," *IEEE Trans. Transport. Electric.*, vol. 6, no. 2, pp. 417-426, 2020.
- [21] C. Wu, C. Zhu, J. Sun, and Y. Ge, "A Synthesized Diagnosis Approach for Lithium-ion Battery in Hybrid Electric Vehicle," *IEEE Trans. Veh. Technol.*, vol. 66, no. 7, pp. 5595-5603, 2017.
- [22] X. Li, Z. Wang, L. Zhang, C. Zou, and D. D. Dorrell, "State-of-health estimation for Li-ion batteries by combining the incremental capacity analysis method with grey relational analysis," *J. Power Sources*, vol. 410-411, pp. 106-114, 2019.
- [23] M. Dubarry, C. Truchot, and B. Y. Liaw, "Cell degradation in commercial LiFePO<sub>4</sub> cells with high-power and high-energy designs," *J. Power Sources*, vol. 258, pp. 408-419, Jul. 2014.
- [24] X. Wu, W. Wang, and J. Du, "Effect of charge rate on capacity degradation of LiFePO<sub>4</sub> power battery at low temperature," *Int. J. Energy Res.*, vol. 44, no. 3, pp. 1775-1788, Mar. 2020.
- [25] J. Tian, R. Xiong, and W. Shen, "State-of-health estimation based on differential temperature for lithium ion batteries," *IEEE Trans. Power Electron.*, vol. 35, no. 10, pp. 10363-10373, 2020.
- [26] X. Bian, Z. Wei, J. He, F. Yan, and L. Liu, "A novel model-based voltage construction method for robust state-of-health estimation of lithium-ion batteries," *IEEE Trans. Ind. Electron.*, 2020.
- [27] X. Feng, J. Li, M. Ouyang, L. Lu, J. Li, and X. He, "Using probability density function to evaluate the state of health of lithium-ion batteries," *J. Power Sources*, vol. 232, pp. 209-218, Jun. 2013.
- [28] S. Torai, M. Nakagomi, S. Yoshitake, S. Yamaguchi, and N. Oyama, "State-of-health estimation of LiFePO<sub>4</sub>/graphite batteries based on a model using differential capacity," *J. Power Sources*, vol. 306, pp. 62-69, Feb. 2016.
- [29] Y. Li *et al.*, "A quick on-line state of health estimation method for Li-ion battery with incremental capacity curves processed by Gaussian filter," *J. Power Sources*, vol. 373, pp. 40-53, 2018.
- [30] X. Li, J. Jiang, L. Y. Wang, D. Chen, Y. Zhang, and C. Zhang, "A capacity model based on charging process for state of health estimation of lithium ion batteries," *Appl. Energy*, vol. 177, pp. 537-543, 2016.
- [31] X. Tang, K. Liu, J. Lu, B. Liu, X. Wang, and F. Gao, "Battery incremental capacity curve extraction by a two-dimensional Luenberger–Gaussian-moving-average filter," *Appl. Energy*, vol. 280, p. 115895, 2020.
- [32] X. Feng *et al.*, "Online state-of-health estimation for Li-ion battery using partial charging segment based on support vector machine," *IEEE Trans. Veh. Technol.*, vol. 68, no. 9, pp. 8583-8592, 2019.
- [33] X. Tang *et al.*, "A fast estimation algorithm for lithium-ion battery state of health," *J. Power Sources*, vol. 396, pp. 453-458, Aug. 2018.
- [34] Z. Yun and W. Qin, "Remaining useful life estimation of lithium-ion batteries based on optimal time series health indicator," *IEEE Access*, vol. 8, pp. 55447-55461, 2020.
- [35] B. Gou, Y. Xu, and X. Feng, "State-of-health estimation and remaining-useful-life prediction for lithium-ion battery using a hybrid data-driven method," *IEEE Trans. Veh. Technol.*, vol. 69, no. 10, pp. 10854-10867, 2020.
- [36] C. Birkil, "Diagnosis and prognosis of degradation in lithium-ion batteries," University of Oxford, 2017.
- [37] David *et al.*, "Lithium-ion battery degradation indicators via incremental capacity analysis," *IEEE Trans. Ind. Appl.*, 2019.
- [38] M. Berecibar, M. Dubarry, I. Villarreal, N. Omar, and J. V. Mierlo, "Degradation mechanisms detection for HP and HE NMC cells based on incremental capacity curves," in *Proc. Veh. Power & Propul. Con.*, 2016.
- [39] X. Hu, J. Jiang, D. Cao, and B. Egardt, "Battery health prognosis for electric vehicles using sample entropy and sparse Bayesian predictive modeling," *IEEE Trans. Ind. Electron.*, 2015.
- [40] J. Li, L. Chao, L. Wang, L. Zhang, and C. Li, "Remaining capacity estimation of Li-ion batteries based on temperature sample entropy and particle filter," *J. Power Sources*, vol. 268, pp. 895-903, Dec. 2014.
- [41] Richman, Joshua, S. Moorman, J. and Randall, "Physiological time-series analysis using approximate entropy and sample entropy," *Amer. J. Physiol. Heart Circ. Physiol.*, 2000.
- [42] W. Chen, Z. Wang, H. Xie, and W. Yu, "Characterization of surface EMG signal based on fuzzy entropy," *IEEE Trans. Neural Syst. Rehabil. Eng.*, vol. 15, no. 2, pp. 266-272, 2007.
- [43] J. M. Yentes, N. Hunt, K. K. Schmid, J. P. Kaipust, D. McGrath, and N. Stergiou, "The appropriate use of approximate entropy and sample entropy with short data sets," *Annals Biomed. Eng.: J. Biomed. Eng. Soc.*, 2013.
- [44] X. Bian, Z. Wei, W. Li, J. Pou, D. U. Sauer, and L. Liu, "State-of-health estimation of lithium-ion batteries by fusing an open-circuit-voltage model and incremental capacity analysis," *IEEE Trans. Power Electron.*, 2021.
- [45] W. Liu, Y. Xu, and X. Feng, "A hierarchical and flexible data-driven method for online state-of-health estimation of Li-Ion battery," *IEEE Trans. Veh. Technol.*, vol. 69, no. 12, pp. 14739-14748, 2020.



**Zhongbao Wei** (M'19–SM'21) received the B.Eng. and the M.Sc. degrees in instrumental science and technology from Beihang University, China, in 2010 and 2013, and the Ph.D. degree in power engineering from Nanyang Technological University, Singapore, in 2017.

He has been a research fellow with Energy Research Institute @ NTU, Nanyang Technological University from 2016 to 2018. He is currently a professor in vehicle engineering with the National Engineering Laboratory for Electric Vehicles, Beijing Institute of Technology, China.

He has authored more than 70 peer-reviewed articles. His research interests include electrified transportation and battery management. He serves as Associate Editor for many international journals like IEEE Transactions on Intelligent Transportation Systems, IET Renewable Power Generation, IET Intelligent Transportation Systems.



**Haokai Ruan** received the B.S. degree in automotive engineering from the Beijing Institute of Technology, Beijing, China, in 2019. He is currently working toward the M.S. degree in mechanical engineering at Beijing Institute of Technology, Beijing, China.

His research interests include the battery state estimation and remaining useful life prediction.



**Yang Li** (S'11–M'16) received the B.E. degree in electrical engineering from Wuhan University, Wuhan, China, in 2007, and the M.Sc. and Ph.D. degrees in power engineering from the Nanyang Technological University (NTU), Singapore, in 2008 and 2015, respectively. From 2015 to 2016, he was a Research Fellow with the Energy Research Institute at NTU (ERI@N), Singapore. From 2016 to 2018, he was a Research Fellow with the School of Electrical Engineering and Computer Science, Queensland University of Technology, Brisbane, Australia. Since 2019, he has been an Associate Professor with the School of Automation, Wuhan University of Technology, Wuhan, China. He is currently a Researcher with the Department of Electrical Engineering, Chalmers University of Technology, Gothenburg, Sweden.

His research interests include modeling, control, and application of renewable and energy storage systems in the power grid and transport sectors. Dr. Li was a recipient of the EU Marie Skłodowska-Curie Individual Fellowship in 2020.



**Jianwei Li** (M'17) received the B.Eng. degree from North China Electric Power University and the Ph.D. degree in Electrical Engineering from the University of Bath, U.K. He has worked with the University of Liege, Beijing Institute of Technology, and the University of Oxford.

His research interests include electrical energy storages and hybrid energy storages, electrical vehicles, connected vehicles, batteries, fuel cells, and power management of the multi-vector system.



**Caizhi Zhang** received the Ph.D. degree in thermal dynamic and fuel cell from the School of Mechanical and Aerospace Engineering, Nanyang Technological University (NTU), Singapore, in 2016.

He joined as a Professor in Chongqing University (CQU), Chongqing, China, in September 2016. Before that, he was a Research Associate and a Research Fellow with NTU. He is currently a Supervisor of doctoral students and the Leader of the Fuel Cell Vehicle Laboratory, School of Automotive Engineering, CQU. He is also a Researcher with the State Key Laboratory of Mechanical Transmissions and the Chongqing Automotive Collaborative Innovation Centre, CQU. He has extensive experience in fuel cell and fuel cell system since September 2008. He participated and in charge of more than ten national-, provincial-, and ministerial-level projects, such as two new energy vehicle projects of the National Key Research and Development Program in 2018 and one project of the Youth National Foundation of China. He has published 70 articles. His research interests are fuel cells, machine learning, and intelligent fuel cell vehicle. Dr. Zhang is the outstanding Reviewer of Energy, Applied Energy, Energy Conversion and Management, and International Journal of Hydrogen Energy.



**Hongwen He** (M'03–SM'12) received the M.Sc. degree from Jilin University of Technology, Changchun, China and the Ph.D. degree from Beijing Institute of Technology, Beijing, China, in 2000 and 2003, respectively, both in vehicle engineering.

He is currently a Professor with the National Engineering Laboratory for Electric Vehicles, School of Mechanical Engineering, Beijing Institute of Technology. Focusing on the research field of "New Energy Vehicle Drive and Control", he has presided over 18 national-level projects/tasks such as the National Key Research and Development Plan for New Energy Vehicles, the National Natural Science Foundation of China (NSFC) etc.

He has published 126 EI-indexed papers, 82 SCI-indexed papers, and 17 ESI highly cited papers. He has been awarded the second prize of the Chinese National Science and Technology Award, the first prize of natural science by the Ministry of Education, the first prize of technological invention of China's automobile industry and the second prize of national defense technology. He received the Best Paper Awards from the journal Energies and the 2017 International Symposium on Electric Vehicles. He is serving in the Editorial Board of Energies and Vehicles. He was the Chair of the 2017 International Conference on Energy, Ecology and Environment held in Stockholm, Sweden.